JOURNAL OF Materials CHEMISTRY

Metal diolates: useful precursors for tailor-made oxides prepared at low temperatures

Heiko Thoms,[a] Matthias Epple,[a] Michael Fröba,[a,b] Joe Wong[b] and Armin Reller *[a†]

[a]*Institute of Inorganic and Applied Chemistry, University of Hamburg, Martin-Luther-King-Platz 6, D-20146 Hamburg, Germany*

[b]*Lawrence Livermore National Laboratory, University of California, P.O. Box 808, L-369, Livermore, CA 94551, USA*

Diolates of titanium and heterometallic diolates of the combinations Mg/Si, Mg/Ti, Mg/Zr and Ti/Si were prepared by reacting alcoholates [*e.g.* $Ti(OC_2H_5)_4$, $Mg(OCH_3)_2{\cdot}CH_3OH$] with α,ω-diols like pentane-1,5-diol. The resulting diolates are probably of polymeric nature and do not form single crystals. Structural information was obtained by infrared spectroscopy, thermal analysis and X-ray absorption spectroscopy at the Mg and Si K-edges. Thermal decomposition of such diolates led to oxides with distinct morphology at comparatively low temperatures (540–800 °C). For the heterometallic diolates the thermal decomposition in most cases led to binary, sometimes metastable oxides. The morphology of the oxides strongly depended on the nature of the precursor.

Introduction

Metal oxides have been used by mankind for more than 4000 years. Ancient cultures used them as colors for paintings or sculptures. Today, oxides find many different applications. For instance, magnesium oxide (MgO) is used as a flame retardant or as an insulator in electrical devices. Titanium dioxide (TiO_2) finds application as catalysts[1] or photocatalysts[2] in organic or metal organic syntheses. It is also extensively used as a white pigment. Zirconium dioxide (ZrO_2) is of importance as a catalyst support or catalyst.[3] The properties of such oxides can be influenced by using different synthetic routes. Metal alcoholates (alkoxides) are interesting precursors for oxides because it is known that they can be decomposed to oxides at moderate temperatures.[4] The morphology and particle size of MgO prepared by thermal decomposition of alcoholates can be strongly influenced by varying the molecular group in the alcoholate.[5–7]

In this work the preparation of diolates of titanium and heterometallic diolates of Mg/Si, Mg/Ti, Mg/Zr and Ti/Si is described. These compounds were thermally decomposed, and the resulting oxides were characterized by scanning electron microscopy and X-ray powder diffraction. The polymeric character of all the diolates prevented single crystal X-ray structure determinations; however, we were able to determine some structural features by X-ray absorption spectroscopy at the Mg and Si K-edges (EXAFS, XANES), and by infrared spectroscopy (IR).

Experimental

Synthesis

Diolates can be prepared from simple metal alcoholates and diols in dry ethanol; *e.g.* for a magnesium–silicon diolate:

$$Mg(OCH_3)_2{\cdot}CH_3OH + Si(OC_2H_5)_4 + 3HO(CH_2)_3OH \rightarrow MgSi[O(CH_2)_3O]_3 + 3CH_3OH + 4C_2H_5OH \quad (1)$$

Note that the chelate effect promotes the desired reaction. Diols were reacted in a small molar excess (10–30% towards the metal) with $Si(OC_2H_5)_4$, $Ti(OC_2H_5)_4$ and $Zr(O^iC_3H_7)_4$, respectively. The mixtures were stirred for 24 h at room temperature, then the products were filtered off and dried *in vacuo* at 40–50 °C for 3 h. The yield was generally high (70–90%). The mixed diolates were moisture-sensitive white powders that mostly were diol adducts. Si-, Ti- and Zr-alcoholates were used as purchased from Merck (Si, Ti) and Fluka (Zr). Magnesium methanolate, $Mg(OCH_3)_2{\cdot}CH_3OH$, was prepared from Mg and methanol as described in ref. 5. The titanium diolates were prepared from $Ti(OC_2H_5)_4$ and the corresponding diol. They were white powders of considerable stability towards moisture [in contrast to $Ti(OC_2H_5)_4$ which hydrolyzes immediately upon contact with moist air]. All procedures were carried out under a dry argon atmosphere. Ethanol was dried with sodium metal.

Analytical data of the diolates (assumed formulae). *$MgSi[O(CH_2)_3O]_3$* ***1***. Yield: 75%. Anal. calc.: C, 39.36, H, 6.56%. Found: C, 39.92, H, 7.18%. Mass loss in TG for decomposition to $SiO_2{\cdot}MgO$: Δm calc. 63.4%, found 68.9%. IR (KBr) ν/cm^{-1}: 3400 (s, O–H str.), 2946/2888 (s, C–H str.), 1618 (m), 1478/1425/1396 (w, C–H def.), 1072 (vs, C–O str.), 985 (m, Si–O), 754 (m, C–C), 446 (m, Mg–O).

$MgTi[O(CH_2)_3O]_3{\cdot}HO(CH_2)_3OH$ ***2***. Yield: 80%. Anal. calc.: C, 36.71, H, 6.12%. Found: C, 38.76, H, 7.57%. Mass loss in TG for decomposition to $MgO{\cdot}TiO_2$: Δm calc. 67.6%, found 68.2%. IR (KBr) ν/cm^{-1}: 3221 (w, O–H str.), 2930/2904/2838 (s, C–H str.), 2709, 1466, 1420, 1378, 1357 (m, C–H def.), 1129/1089 (vs, C–O str.), 932 (m, Ti–O), 838 (m, C–C), 571 (s, Ti–O), 497 (s, Mg–O).

$MgZr[O(CH_2)_3O]_3{\cdot}1.3HO(CH_2)_3OH$ ***3***. Yield: 83%. Anal. calc.: C, 35.48, H, 6.51%. Found: C, 35.28, H, 6.69%. Mass loss in TG for decomposition to $MgO{\cdot}ZrO_2$: Δm calc. 62.6%, found 60.1%. IR (KBr) ν/cm^{-1}: 3210 (w, O–H str.), 2930/2900/2845 (s, C–H str.), 1466, 1420, 1384 (m, C–H def.), 1133, 1090 (vs, C–O str.), 969, 938 (m, Zr–O), 829 (m, C–C), 546 (s, Mg–O).

$Mg_2Si[O(CH_2)_3O]_4{\cdot}HO(CH_2)_3OH$ ***4***. Yield: 82%. Anal. calc.: C, 40.12, H, 7.13%. Found: C, 40.57, H, 7.48%. Mass loss in TG for decomposition to 2 $MgO{\cdot}SiO_2$: Δm calc. 68.7%, found 72.0%. IR (KBr) ν/cm^{-1}: 3364 (m, O–H str.), 2946/2884 (s, C–H str.), 1618 (m), 1477, 1424, 1391 (w, C–H def.), 1091 (vs, C–O str.), 986 (m, Si–O), 951, 818, 751 (m, C–C), 489 (m, Mg–O).

†E-mail: reller@xray.chemie.uni-hamburg.de.

$MgSi[O(CH_2)_4O]_3{\cdot}2HO(CH_2)_4OH$ ***5***. Yield: 70%. Anal. calc.: C, 48.35, H, 8.86%. Found: C, 49.57, H, 9.32%. Mass loss in TG for decomposition to $MgO{\cdot}SiO_2$: Δm calc. 79.8%, found 80.8%. IR (KBr) ν/cm^{-1}: 3399 (s, O–H str.), 2942/2879 (s, C–H str.), 1652 (m), 1479, 1448, 1394 (w, C–H def.), 1099 (vs, C–O str.), 1021, 985 (m, Si–O), 856, 740 (m, C–C), 528–413 (m, Si–O, Mg–O).

$SiTi[O(CH_2)_3O]_4{\cdot}2HO(CH_2)_3OH$ ***6***. Yield: 84%. Anal. calc.: C, 41.21, H, 7.63%. Found: C, 40.20, H, 7.33%. Mass loss in TG for decomposition to $SiO_2{\cdot}TiO_2$: Δm calc. 73.3%, found 71.4%. IR (KBr) ν/cm^{-1}: 3430 (m, O–H str.), 2936/2882/2842 (s, C–H str.), 1476, 1422, 1379 (m, C–H def.), 1091 (vs, C–O str.), 986, 928 (m, Si–O–Ti), 841 (m, C–C), 608 (m).

$Ti[O(CH_2)_2O]_2{\cdot}0.3HO(CH_2)_2OH$ ***7***. Yield: 84%. Anal. calc.: C, 29.60, H, 5.25%. Found: C, 30.71, H, 5.66%. Mass loss in TG for decomposition to TiO_2: Δm calc. 57.2%, found 57.5%. IR (KBr) ν/cm^{-1}: 3368 (m, O–H str.), 2924 (s, C–H str.), 1457, 1354 (m, C–H def.), 1119, 1062 (vs, C–O str.), 913, 884 (s, C–C), 614 (s, Ti–O).

$Ti[O(CH_2)_3O]_2$ ***8***. Yield: 95%. Anal. calc.: C, 36.75, H, 6.13%. Found: C, 36.65, H, 6.50%. Mass loss in TG for decomposition to TiO_2: Δm calc. 59.2%, found 61.2%. IR (KBr) ν/cm^{-1}: 3391, 3326 (m, O–H str.), 2938/2856 (s, C–H str.), 1467, 1370 (m, C–H def.), 1063, 1021 (vs, C–O str.), 918, 870, 824 (w, C–C), 599 (s, Ti–O).

$Ti[O(CH_2)_4O]_2{\cdot}0.5HO(CH_2)_4OH$ ***9***. Yield: 91%. Anal. calc.: C, 44.63, H, 7.81%. Found: C, 44.87, H, 8.09%. Mass loss in TG for decomposition to TiO_2: Δm calc. 70.3%, found: 70.5%. IR (KBr) ν/cm^{-1}: 3391 (m, O–H str.), 2931/2867 (s, C–H str.), 1431, 1376 (m, C–H def.), 1102, 1052, 1025 (vs, C–O str.), 946 (w, C–C), 609 (m, Ti–O).

$Ti[O(CH_2)_5O]_2$ ***10***. Yield: 94%. Anal. calc.: C, 47.64, H, 7.94%. Found: C, 48.05, H, 8.63%. Mass loss in TG for decomposition to TiO_2: Δm calc. 68.3%, found 70.0%. IR (KBr) ν/cm^{-1}: 3352 (m, O–H str.), 2929/2857 (s, C–H str.), 1466/1374 (m, C–H def.), 1078 (vs, C–O str.), 895 (w, C–C), 594 (s, Ti–O).

$Ti[O(CH_2)_6O]_2{\cdot}0.5HO(CH_2)_6OH$ ***11***. Yield: 92%. Anal. calc.: C, 53.25, H, 9.17%. Found: C, 53.05, H, 9.36%. Mass loss in TG for decomposition to TiO_2: Δm calc. 76.4%, found 76.7%. IR (KBr) ν/cm^{-1}: 3392 (m, O–H str.), 2932, 2856 (s, C–H str.), 1466, 1371 (m, C–H def.), 1061 (vs, C–O str.), 1022 (w, C–C), 604 (m, Ti–O).

$Ti[O(CH_2)_8O]_2$ ***12***. Yield: 96%. Anal. calc.: C, 57.16, H, 9.53%. Found: C, 56.98, H, 9.66%. Mass loss in TG for decomposition to TiO_2: Δm calc. 76.2%, found 76.1%. IR (KBr) ν/cm^{-1}: 3400/3334 (m, O–H str.), 2926/2852 (s, C–H str.), 1462, 1359 (m, C–H def.), 1050 (s, C–O str.), 984 (w, C–C), 604 (m, Ti–O).

Methods of characterization

IR spectra were measured on a Perkin-Elmer FT-IR 1720. The thermochemical behavior of all samples was studied with a simultaneous thermal analyzer (Netzsch STA 409C/MS) which records DTA, thermogravimetry and evolved reaction gases by mass spectrometry (Balzers QMS 421). The samples were heated in open alumina crucibles in a dynamic air atmosphere (50 ml min^{-1}) with a heating rate of 10 K min^{-1}. The typical sample mass was 50–200 mg. SEM analyses were performed with a Philips SEM 515 scanning electron microscope. X-Ray powder diffraction was carried out with a Philips PW1049 powder diffractometer (Cu-Kα radiation). X-Ray absorption spectroscopy at the Si K-edge was carried out at the LURE synchrotron (Paris, France; ring Superaco: 800 MeV and 200–400 mA). Beamline SA 32 was used with an InSb monochromator. The sample was measured in the range between 1800 and 2400 eV with a counting time of 1 s and a step width of 1 eV. Mg K-edge spectra were recorded at the Stanford Synchrotron Radiation Laboratory (SSRL, Stanford, USA; ring SPEAR: 3 GeV and 100 mA) at the JUMBO beamline 3-3 equipped with a YB_{66} (400) double-crystal monochromator.[8–10]

All spectra were taken at room temperature as polyethylene pellets. The edges were calibrated against the pure elements (Mg K-edge: 1303 eV, Si K-edge: 1838 eV). A pre-edge fit was applied and the spectra were normalized to an edge jump of 1. All data analysis procedures were carried out using the programs WINXAS[11] and FEFF.[12,13]

Results and Discussion

Thermal decomposition to oxides

The thermal decomposition of the assumed heterometallic diolates in air or oxygen led to binary oxides. Further annealing for 18 h at 850 °C in air led to crystallization in some cases. The results are shown in Table 1.

The thermal decomposition of the six titanium diolates in oxygen (700 °C) led in all cases to a mixture of the TiO_2 polymorphs anatase and rutile. No trend in the proportion of either phase was observed. Interestingly, the final decomposition temperature notably decreased with increasing carbon chain length of the precursor diolate (Fig. 1). This is opposite to the effect observed with magnesium diolates of different carbon chain length.[6] The final decomposition temperature is defined here as the temperature at which the mass loss has ceased and no further gaseous products are detected by mass spectrometry.

Titanium bis(ethane-1,2-diolate)·0.3ethane-1,2-diol **7** decomposes to TiO_2 at *ca.* 510 °C, titanium bis(octane-1,8-diolate) **12** decomposes at *ca.* 410 °C. The TG-MS diagrams in Fig. 2(a) and (b) demonstrate the different amounts of diol in the diolate. Titanium bis(ethane-1,2-diolate)·0.3ethane-1,2-diol **7** shows more degradation steps than titanium bis(pentane-1,5-diolate) **10** because it contains 0.3 molecules of diol that are

Table 1 Final decomposition temperatures and resulting oxides after thermal decomposition of the mixed diolates

compound	final decomposition temperature to oxides	resulting oxides after thermal decomposition/after further annealing for 18 h at 850 °C
$MgSi[O(CH_2)_3O]_3$ **1**	800 °C (air) 600 °C (O_2)	amorphous/$MgSiO_3$
$MgTi[O(CH_2)_3O]_3{\cdot}HO(CH_2)_3OH$ **2**	740 °C (air)	$MgTiO_3$/$MgTiO_3$ and $MgTi_2O_5$[a]
$MgZr[O(CH_2)_3O]_3{\cdot}1.3HO(CH_2)_3OH$ **3**	780 °C (air)	$MgZr_5O_{12}$[a]/$MgZr_5O_{12}$[a]
$Mg_2Si[O(CH_2)_3O]_4{\cdot}HO(CH_2)_3OH$ **4**	600 °C (O_2)	amorphous[a]/Mg_2SiO_4
$MgSi[O(CH_2)_4O]_3{\cdot}2HO(CH_2)_4OH$ **5**	600 °C (O_2)	amorphous[a]/Mg_2SiO_4[a]
$SiTi[O(CH_2)_3O]_4{\cdot}2HO(CH_2)_3OH$ **6**	540 °C (O_2)	TiO_2 (anatase)/TiO_2 (anatase and rutile)[a]

[a]The missing stoichiometric amounts of MgO and SiO_2 are assumed to be amorphous.

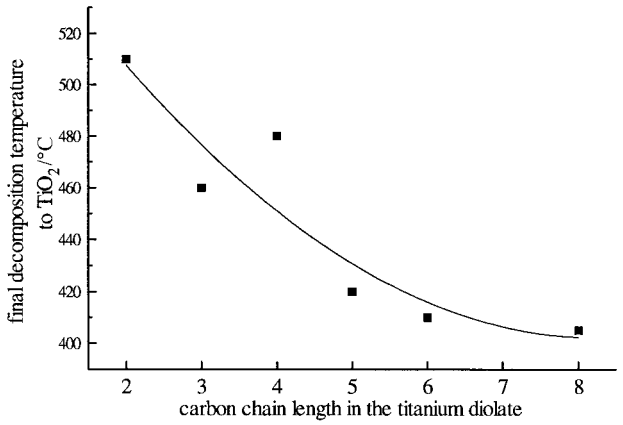

Fig. 1 Decrease of the final decomposition temperature of the titanium diolates with increasing diolate chain length

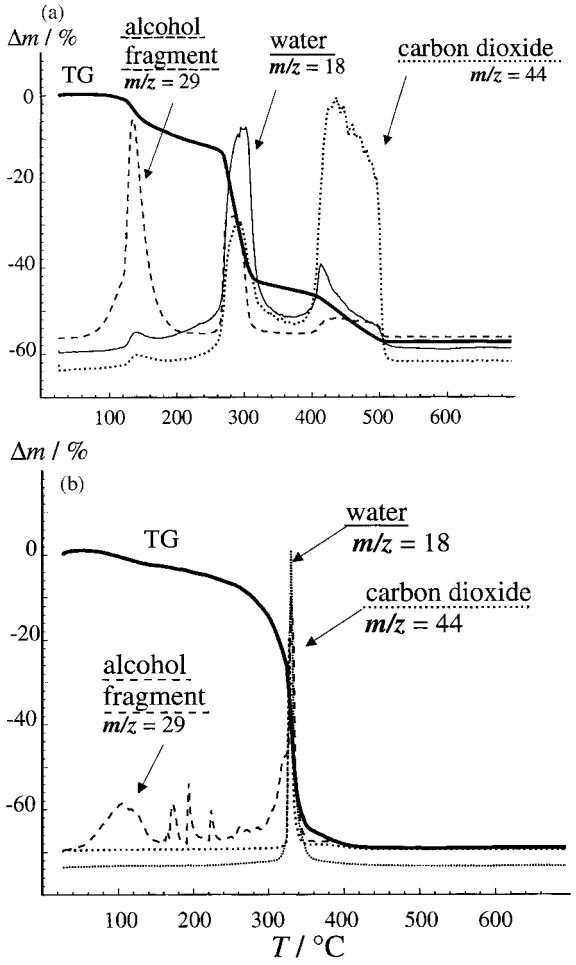

Fig. 2 TG-MS diagrams of (a) $Ti[O(CH_2)_2O]_2 \cdot 0.3HO(CH_2)_2OH$ **7** in O_2 and (b) $Ti[O(CH_2)_5O]_2$ **10** in O_2; not all gaseous products are shown

evolved first upon heating [Δm(calc.) for 0.3 mol diolate: 10.8%; found: *ca.* 12%].

Structural aspects

The highly polymeric character of the diolates (which is known for many simple alcoholates)[4,14] prevented the growth of single crystals. However, we were able to extract some structural aspects of the diolates by using alternate methods. EXAFS spectroscopy (extended X-ray absorption fine structure) is a useful method to obtain structural information for crystalline and amorphous materials.[15] EXAFS spectroscopy was carried out at the Si K-edge on magnesium–silicon tris(propane-1,3-diolate) **1**. Fourier transformation (k-range 2 to 12 $Å^{-1}$, k^3-weighting) gives the modified radial distribution function that shows the coordination sphere around silicon in the distance r' (Fig. 3). The spectra were fitted with theoretical phases and amplitudes of a SiO_4–Mg cluster. The first shell, oxygen coordination around silicon, was refined. The refinement gave four oxygen atoms in a distance of 1.62 Å, a typical bond length for an Si–O group.[16] The Debye–Waller factor was $\Delta\sigma^2 = 0.00163$ $Å^2$. The second shell that represents the magnesium ion was obtained during the fit with a fixed coordination number of 1, a fixed distance of 2.345 Å and a fixed Debye–Waller factor of $\Delta\sigma^2 = 0.0045$ $Å^2$. Fig. 3 shows the measured spectrum (solid line) and the calculated spectrum (dotted line) for this $(SiO)_4$–Mg group. The similarity of the spectra suggests that the substance is really a heterometallic diolate, with magnesium and silicon bridged by oxygen. Fits of carbon in the second coordination sphere were not successful.

Recently, we reported on main structural elements of the crystalline magnesium methanolate solvate complex $Mg(OCH_3)_2 \cdot 2CH_3OH$ by single crystal X-ray structure determination.[17] In this case, the molecular units are heterocubanes with Mg^{2+} and OCH_3^- ions in the corners. The Mg ions are surrounded by distorted oxygen octahedra. The insolubility of all magnesium alcoholates prevented the application of many analytical tools, like NMR spectroscopy in solution or UV spectroscopy. However, to understand the thermal decomposition pathway from the alcoholates to the oxides it is important to know the structures of the alcoholates and intermediates. X-Ray absorption spectroscopy at the Mg K-edge is a possible way to obtain this information.[10,18,19]

As an example, we chose magnesium ethanolate $Mg(OC_2H_5)_2$, the structure of which is still unknown.[5] When heated in air, the substance decomposes in two steps at 285 °C and 350 °C to MgO. *Ex situ* IR spectroscopy of intermediates taken during the thermal decomposition showed a new absorption band at 1620 cm^{-1} that was attributed (in combination with elemental analysis) to alkoxy–hydroxy intermediates of the general formula $Mg(OC_2H_5)_{2-x}(OH)_x$. It appears likely that the decomposition occurs *via* a successive replacement of alkoxy groups by hydroxy groups. We tried to confirm this assumption by X-ray absorption spectroscopy.

The XANES spectrum of $Mg(OC_2H_5)_2$ shows a triplet structure between 1310 eV and 1320 eV (Fig. 4, spectrum 1) that is typical for MgO_6 octahedra like in $Mg(OH)_2$.[10,18,19] This indicates that the direct coordination of the Mg ion in $Mg(OC_2H_5)_2$ is similar to that in $Mg(OCH_3)_2 \cdot 2CH_3OH$: the Mg ion is surrounded by an oxygen octahedron.

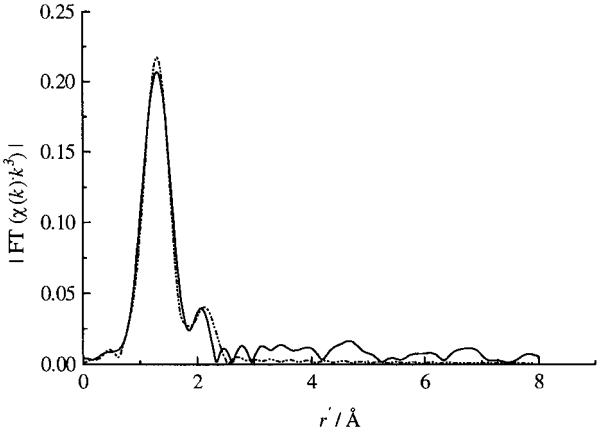

Fig. 3 Si K-edge EXAFS: Fourier transform magnitude of $MgSi[O(CH_2)_3O]_3$ **1** (solid line) and of a theoretical SiO_4–Mg cluster (dotted line)

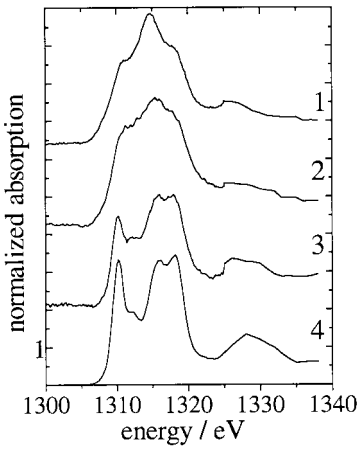

Fig. 4 Mg K-edge XANES: X-ray absorption spectroscopy (room temperature) on magnesium ethanolate $Mg(OCH_2CH_3)$ and its intermediates on the way to MgO: 1, $Mg(OC_2H_5)_2$; 2, the first intermediate $Mg(OC_2H_5)(OH)$, taken at 285 °C; 3, the second intermediate $Mg(OC_2H_5)_{0.25}(OH)_{1.75}$, taken at 350 °C; 4, pure magnesium oxide MgO

The XANES spectrum of the first thermal intermediate $Mg(OC_2H_5)(OH)$ taken at 285 °C shows similar features (spectrum 2), but the triplet structure is more smeared out due to a higher degree of distortion in the surrounding coordination shells. In contrast, the second intermediate $Mg(OC_2H_5)_{0.25}(OH)_{1.75}$ taken at 350 °C already shows a XANES spectrum (spectrum 3) very similar to that of MgO (spectrum 4),[10,18,19] the final product of the thermal decomposition. MgO crystallizes in the NaCl structure with magnesium in octahedral coordination. The XANES spectrum of the second intermediate with its typical 'MgO features' suggests that the substance already has a distorted NaCl structure.

This study of $Mg(OC_2H_5)_2$ and its intermediates demonstrates that the principal coordination of magnesium does not change during the thermal decomposition in air; the magnesium ion is always surrounded by an oxygen octahedron. The coordination geometry remains unchanged during the reaction, *i.e.*, we probably have a nanoscale topotactic reaction. Similar results have been found in a XANES study that investigated the process of MgO formation by dehydration of $Mg(OH)_2$.[18] The use of $Mg(OC_2H_5)_2$ as a precursor for MgO has been described in ref. 17.

IR spectroscopy gave some structural information about the prepared titanium diolates. The Ti–O absorption band of $Ti(OC_2H_5)_4$ is at *ca.* 580 cm^{-1}, whereas for the examined titanium diolates it was found at *ca.* 610 cm^{-1} (Fig. 5). This suggests that the diolates have a more covalent bond character.

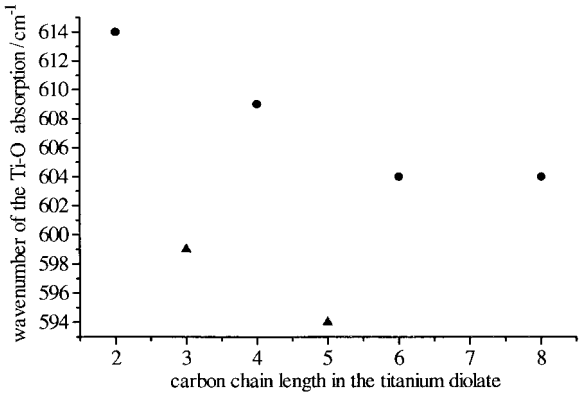

Fig. 5 Change of the Ti–O absorption in the IR spectra of the titanium diolates; the absorption band of $Ti(OC_2H_5)_4$ is at 580 cm^{-1}

This result corresponds well with other properties of titanium diolates, which are colorless substances and insoluble in all applied solvents. The structure of these diolates may be a polymeric network in which the Ti^{4+} ion is surrounded by bridging diolate groups.

Fig. 5 shows another aspect: the Ti–O absorption band of the diolates with carbon chain lengths of 3 and 5 is found at a significantly lower wavenumber than the absorption band of the diolates with carbon chain lengths of 2, 4, 6 and 8. This may be interpreted as a possible structural difference because of a different orientation of the methylene chains in the solid state.

Morphology of the oxides

The thermal decomposition of the metal diolates led to metal oxides with distinct morphology. Scanning electron microscopy showed that particle size and porosity strongly depend on the precursor diolate. $MgSiO_3$ from magnesium–silicon tris (propane-1,3-diolate) is composed of bulky particles with spherical indentations [Fig. 6(a)]; however, the product from $SiTi[O(CH_2)_3O]_4{\cdot}2HO(CH_2)_3OH$ **6** shows a porous morphology with pores in the range of 5 to 2 μm [Fig. 6(b)].

TiO_2 prepared from thermal decomposition of the titanium diolates shows significant differences in morphology as a function of the precursor diolate [Fig. 7(a)–(c)]. With increasing carbon chain length in the precursor the morphology of the titanium oxides changes from curved [Fig. 7(a)] over a morphology with cavities and spherical holes [Fig. 7(b)] to an oxide with skeleton-like regions [Fig. 7(c)]. Obviously, by

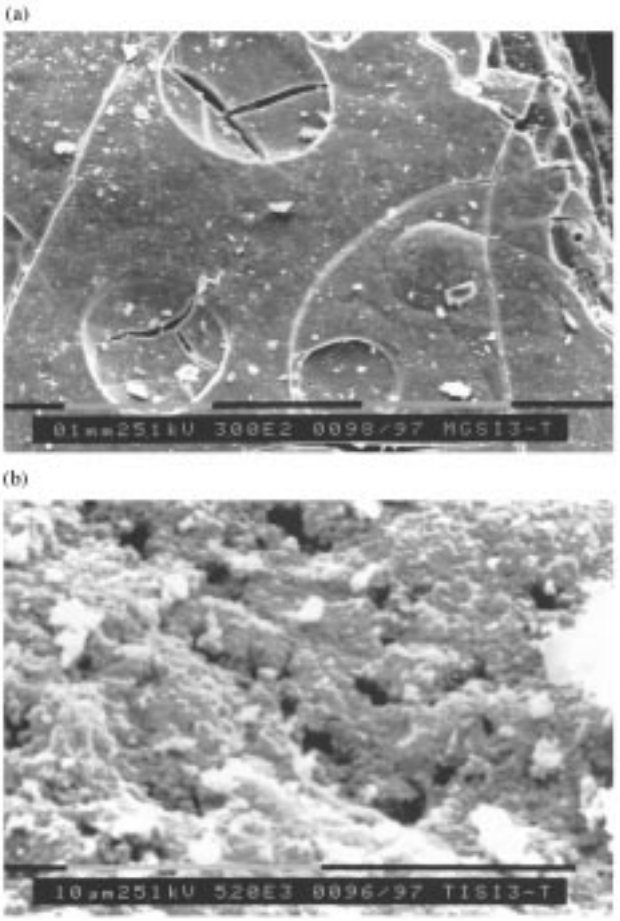

Fig. 6 Selected scanning electron micrographs of binary oxides (prepared from heterometallic diolates): (a) $MgSiO_3$ from $MgSi[O(CH_2)_3O]_3$ **1** (300×); (b) TiO_2/SiO_2 from $SiTi[O(CH_2)_3O]_4{\cdot}2HO(CH_2)_3OH$ **6** (5200×)

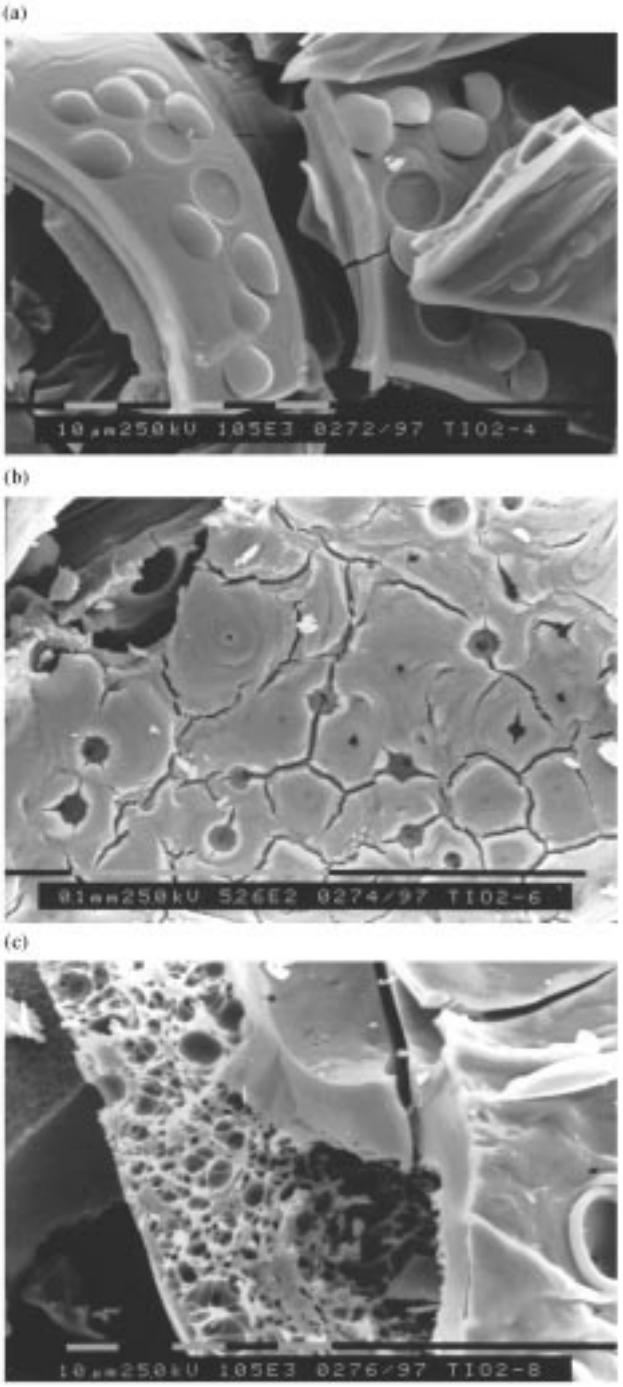

Fig. 7 Scanning electron micrographs of titanium oxides (TiO_2) prepared from titanium diolates at 700 °C: (a) precursor $Ti[O(CH_2)_4O]_2 \cdot 0.5HO(CH_2)_4OH$ **9** (1050×); (b) precursor $Ti[O(CH_2)_6O]_2$ **11** (526×); (c) precursor $Ti[O(CH_2)_8O]_2$ **12** (1050×)

increasing the size of the precursor diolate the resulting TiO_2 becomes more and more hollow, probably because of the increasingly bulky organic groups that leave the structure during the thermal decomposition.

Conventionally, titanium dioxide is prepared by hydrolysis of titanium(IV) alcoholates[20] or titanium(IV) salts like $Ti(SO_4)_2$.[21] Kim and Park generated titania particles by thermal decomposition of a mixture of titanium tetraisopropanolate and *tert*-butanol in an aerosol reactor.[22] The resulting particle sizes were between 40 and 80 nm, depending on the ratio of alcoholate to alcohol. To our knowledge, titanium diolates have not yet been used to prepare titania with distinct morphology.

Conclusions

We have shown that metal diolates that can be prepared from simple alcoholates are suitable precursors for oxides. They decompose to oxides at comparatively low temperatures (between 400 °C and 800 °C). It is also possible to obtain oxides with different morphology by varying the precursor diolate. Structural information about the highly polymeric diolates and alcoholates was obtained by using X-ray absorption spectroscopy at the Mg and Si K-edges.

We thank the Deutsche Forschungsgemeinschaft DFG and the Fonds der Chemischen Industrie for generous financial support. We thank Prof. Lechert, Hamburg, for the permission to use the scanning electron microscope. We are grateful to Dr. Flank and Dr. Lagarde at the LURE synchrotron for help during the measurements of the EXAFS spectra.

M.F. thanks the Alexander-von-Humboldt foundation for a Feodor-Lynen Research Fellowship. The work in Livermore, CA, USA, was performed under the auspices of the US Department of Energy (DOE) by the Lawrence Livermore National Laboratory under contract number W-7405-ENG-48. The measurements of the Mg K-edge XANES spectra were carried out at SSRL which is supported by the Chemical Sciences Division of the DOE.

References

1 R. Murugavel and H. W. Roesky, *Angew. Chem.*, 1997, **109**, 491.
2 V. Augugliaro, V. Loddo, G. Marci, L. Palmisano and M. J. Lopez-Munez, *J. Catal.*, 1997, **166**, 272.
3 Z. Feng, W. S. Postula, C. Erkey, C. V. Philip, A. Akgerman and R. G. Anthony, *J. Catal.*, 1994, **148**, 84.
4 D. C. Bradley, *Chem. Rev.*, 1989, **89**, 1317.
5 H. Thoms, M. Epple and A. Reller, *Solid State Ionics*, 1997, **101–103**, 79.
6 H. Thoms, M. Epple and A. Reller, *Thermochim. Acta*, 1997, **302**, 195.
7 H. Thoms, PhD Thesis, University of Hamburg, 1997.
8 J. Wong, G. Shimkaveg, W. Goldstein, M. Eckart, T. Tanaka, Z. U. Rek and H. Tompkins, *Nucl. Instrum. Methods A*, 1990, **291**, 243.
9 M. Rowen, Z. U. Rek, J. Wong, T. Tanaka, G. N. George, I. J. Pickering, G. H. Via and G. E. Brown Jr., *Synchrotron Radiat. News*, 1993, **6**, 25.
10 J. Wong, G. N. George, I. J. Pickering, Z. U. Rek, M. Rowen, T. Tanaka, G. H. Via, B. DeVries, D. E. W. Vaughan and G. E. Brown Jr., *Solid State Commun.*, 1994, **92**, 559.
11 T. Reßler, *J. Phys. IV* (*Coll.*), 1997, **7**, C2.
12 J. J. Rehr, R. C. Albers and S. I. Zabinsky, *Phys. Rev. Lett.*, 1992, **69**, 3397.
13 E. A. Stern, M. Newville, B. Ravel, Y. Yacoby and D. Haskel, *Physica B*, 1995, **208–209**, 117.
14 D. C. Bradley, R. C. Mehrotra and D. P. Gaur, *Metal alkoxides*, Academic Press, London, 1978.
15 H. Bertagnolli and T. S. Ertel, *Angew. Chem.*, 1994, **106**, 15.
16 W. H. Baur, *Trans. Am. Crystallogr. Assoc.*, 1970, **6**, 129.
17 H. Thoms, M. Epple, H. Viebrock and A. Reller, *J. Mater. Chem.*, 1995, **5**, 589.
18 T. Yoshida, T. Tanaka, H. Yoshida, S. Takenaka, T. Funabiki, S. Yoshida and T. Murata, *Physica B*, 1995, **209**, 581.
19 P. Ildefonse, G. Calas, A. M. Flank and P. Lagarde, *Nucl. Instrum. Methods B*, 1995, **97**, 172.
20 T. Mineo, M. Aihara, A. Tsutsumi and K. Yoshida, *Kagaku Kogaku Ronbunshu*, 1996, **2**, 408.
21 H. K. Park, Y. T. Moon, D. K. Kim and C. H. Kim, *J. Am. Ceram. Soc.*, 1996, **10**, 2727.
22 K. Y. Kim and S. B. Park, *J. Chem. Eng. Jpn.*, 1994, **5**, 657.

Paper 8/01263F; *Received* 13*th February*, 1998